Int. Journ. of Peening Science and Technology, Vol. 1, pp. 221–232
Reprints available directly from the publisher
Photocopying permitted by license only.

Evaluation of Surface Properties of Silicon Nitride Ceramics Treated with Laser Peening

K. SAIGUSA[1], K. TAKAHASHI [1]* AND N. SIBUYA[2]

[1]*Faculty of Engineering, Yokohama National University, 79-5 Tokiwadai, Hodogaya-ku, Yokohama-shi, Kanagawa, Japan*
[2]*Sintokogio, LTD, 71-2 Tsukeda, Nishijo, Oharu-cho, Ama-gun, Aichi, Japan*

Laser peening (LP) is a process that has been mainly applied to metals. However, few studies have applied LP to ceramics. In this study, laser peening without coating (LPwC) was applied to silicon nitride reinforced with silicon carbide (Si_3N_4/SiC). Smooth, laser-peened, and shot-peened specimens were prepared, and the surface conditions, surface roughness, and residual stresses were investigated. The surface roughness increased after LP due to laser ablation. When the LP parameters such as power density and coverage were too high, cracks initiated on the surface. Further, when appropriate LP parameters were selected, a compressive residual stress of up to 230 MPa was introduced on the surface and the depth was about 50 μm. Although the magnitude of the surface residual stress of the laser-peened specimen was smaller than that of the shot-peened specimen, LP was able to introduce a deeper compressive residual stress.

Keywords: Laser peening, silicon nitride, ceramics, residual stress, surface roughness, surface properties

1 INTRODUCTION

Ceramics have excellent properties compared to metals, such as heat shock resistance, ablation resistance, and corrosion resistance. Therefore, ceramics are used in various applications. However, ceramic materials are brittle. Thus, their fracture toughness is much lower than that of metals.

To address this problem, many studies have been conducted with the goal of increasing the strength of ceramics by controlling their microstructures

Corresponding author's e-mail: takahashi-koji-ph@ynu.ac.jp

and developing composite materials. In addition, surface treatments have also been studied. Shot peening (SP) is a technique used to introduce compressive residual stress by hitting small shot materials against the surface of the target material. In recent years, the effects of SP on ceramics have been studied by several researchers [1–8]. Ito et al. reported that the bending strength of partially stabilized zirconia (PSZ) increased after SP [1]. Moon et al. reported that a compressive residual stress was introduced by SP on the surface of silicon nitride, which improved the apparent fracture toughness [2]. Tanaka et al. reported that a compressive residual stress was introduced in silicon nitride by fine-particle peening and ultrasonic peening, resulting in improved apparent fracture toughness [3]. Pfeiffer et al. also reported that the compressive residual stress introduced by SP increased the static and cyclic load capacities of alumina and silicon nitride [4]. Takahashi et al. reported that improvements in the apparent fracture toughness and contact strength of a Si_3N_4/SiC composite material were achieved by SP [5]. Takahashi et al. also showed that the bending strength and abrasion resistance of PSZ increased due to the effects of the compressive residual stress induced by SP [6, 7]. Shukla reported that the surface fracture toughness of a zirconia-advanced ceramic increased by micro-shot peening [8]. However, due to the physical contact with the shot material during SP, there is a possibility of surface peeling or chipping, which can result in large decreases in strength.

Therefore, we focused on laser peening (LP) in this study. LP is a technique that utilizes the impact force of plasma generated by the irradiation of a pulsed laser. LP is used for preventing many forms of damage, such as fatigue, wear, and stress corrosion cracking (SCC) in metals. For example, introduction of residual stress and improvement of the fatigue performances of metal components by LP were reported [9]. Sano et al. investigated the residual stress improvement in the surface of SUS304 by laser irradiation [10]. In addition, the application of LP to various materials has been studied. For example, retardation of crack initiation in austenitic stainless steels [11] and improvement in the fatigue life of a titanium alloy [12] were reported. Moreover, stress corrosion cracking resistance and significant decreases in fatigue crack growth rates in aluminum alloy welded joints were reported [13, 14]. Further, introduction of residual stress and improvement of the fatigue strength of a nickel-based alloy were reported [15].

Further, the effects of LP on ceramics have been studied as follows. Akita et al. reported that compressive residual stresses up to 270 MPa could be introduced by applying LP to silicon nitride. They also reported that the bending strengths of laser-peened specimens were improved compared to those of smooth specimens [16]. Shukla et al. reported that LP improved the hardness and fracture toughness of alumina [17] and silicon carbide [18], and that compressive residual stresses were introduced to Al_2O_3 armor ceramics [19]. In addition, Shukla and Lawrence applied LP to Si_3N_4 advanced ceramics and reported an improvement in fracture toughness [20, 21]. Shukla sum-

marized the results of LP of ceramics in recent years [22]. Wang et al. applied LP to Al_2O_3 ceramics and reported that compressive residual stresses of up to 671 MPa were introduced on the surface with a depth of about 1.2 mm [23]. Wang et al. also reported that compressive residual stresses of 850~900 MPa were generated on the surface of Al_2O_3 ceramics by LP, and were retained on the surface after annealing for 10 h at 1100 ºC and 1300 ºC [24]. Xing et al. found that femtosecond LP improved the wear resistance of Al_2O_3/TiC cutting tools [25].

As mentioned above, many studies have applied LP to metals. However, the application of LP to ceramics has been limited because of the concerns regarding the formation of micro-cracks under the strong LP conditions required to introduce large compressive residual stresses. Therefore, when LP is applied to ceramics, it is necessary to investigate the relationship between LP and the surface conditions.

In this study, we applied LP to silicon nitride reinforced with silicon carbide (Si_3N_4/SiC) and investigated its surface properties such as the surface roughness and residual stress distribution. Finally, we determined the appropriate LP conditions for Si_3N_4/SiC.

2 EXPERIMENTAL PROCEDURES

2.1 Materials and specimens

In this study, we used silicon nitride reinforced with silicon carbide (Si_3N_4 / SiC). The samples were prepared using a mixture of Si_3N_4 with 20 wt% SiC powder and 8 wt% Y_2O_3 as a sintering additive. The mixed powders were dried and subsequently hot-pressed at 1850 °C and 35 MPa for 2 h in a N_2 atmosphere. Detailed methods for preparing the test materials were reported previously [26]. The hot-pressed plates were then cut into test specimens measuring 3 mm × 4 mm × 40 mm. One face of each specimen was ground with a grindstone and polished with a 6 μm diamond slurry to a mirror-like finish. The arithmetic average surface roughness (R_a) was 0.025 μm. One of the edges of the specimen was chamfered. This specimen is denoted as the "smooth specimen."

2.2 Laser peening process

Laser peening without coating (LPwC) was applied to the smooth specimens in water. Table 1 lists the conditions of the LP process. The second harmonic of a Q-switched Nd:YAG laser (λ = 532 nm, SAGA, Thales, France) was used. The pulse duration (t) was 6.2 ns and the repetition rate was 10 Hz. The spot diameter of the laser (D) was fixed as 0.5 mm. The pulse energy (E_p) indicates the energy contained per pulse of the laser. The irradiation density (N_p) indicates the number of pulses irradiated per unit area. The peak power

TABLE 1
Conditions of laser peening.

Specimens	Pulse energy, E_p [mJ]	Spot diameter, D [mm]	Power density, G [GW/cm^2]	Irradiation density, N_p [Pulse/mm^2]	Overlapping pitch [mm]	Overlap ratio [%]	Coverage, C_v [%]
Specimen 1	24	0.5	2	16	0.25	50	314
				51	0.14	72	1000
				153	0.081	84	3000
				255	0.063	87	5000
Specimen 2	194		16	16	0.25	50	314
				51	0.14	72	1000
				153	0.081	84	3000
				255	0.063	87	5000
Specimen 3	401		33	16	0.25	50	314
				51	0.14	72	1000
				153	0.081	84	3000
				255	0.063	87	5000

density (G), which is the light intensity per unit area, can be calculated by the following equation using the pulse energy, E_p, and spot area, A_p (= $\pi d^2/4$):

$$G = \frac{E_p}{A_p t} \tag{1}$$

Three power densities, G = 2, 16, and 33 GW/cm^2, were selected.

Figure 1(a) shows the peening area of the specimen, and Figure 1(b) shows the peening pattern and laser track in the laser-peened area. Figure 1(c) shows the experimental setup of LP. The specimens were submerged in a water bath, and then processed by LP. The laser was rastered over the specimens in the y (width) direction followed by shifting in the x (longitudinal) direction in one layer. The pitches of the laser spot were ranged from 0.063 to 0.25 mm, and the corresponding overlap ratios were 50% to 87%. The pitch is the distance between two laser-irradiated spots. In Figure 1(c), the pitch in the x direction is the same as the pitch in the y direction.

The coverage, C_v, which is the amount of overlap per unit area, is calculated by the following equation proposed by Sano et al. [10] using the irradiation density, N_p, and spot area, A_p:

$$C_v = N_p A_p \tag{2}$$

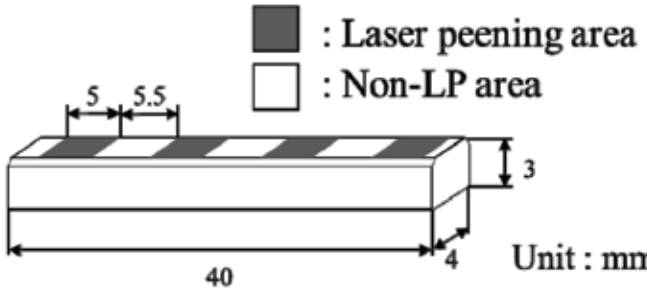

(a) Laster peening area of the specimen

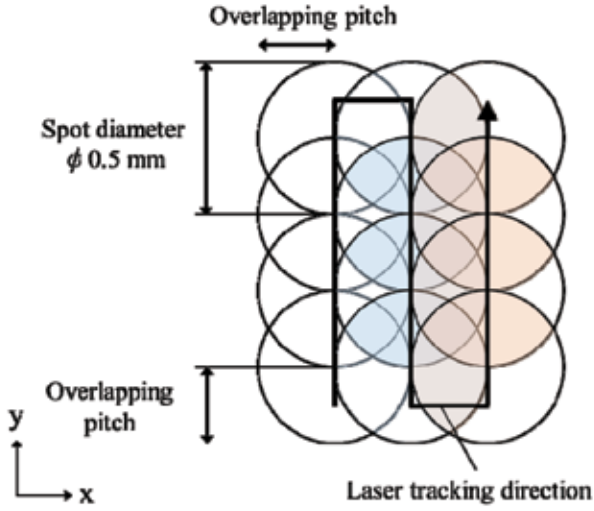

(b) Peening pattern and laser track in the laser peening area

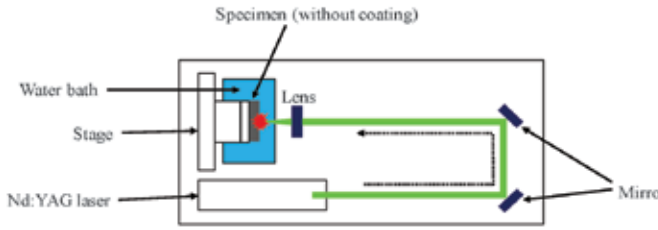

(c) Experimental setup of laser peening

FIGURE 1
Schematic diagram of peening method applied to the specimen.

Here, C_v = 314, 1000, 3000, and 5000% were selected. In this LP, we constructed 1 path. In this study, shot-peened specimens were also prepared for comparison. In SP, the shot diameter was 300 μm and the shot pressure was 0.2 MPa [5].

2.3 Measurement of surface condition, surface roughness, and residual stress

Surface observations and surface roughness measurements of the specimens were carried out using an optical microscope and a stylus-type surface roughness-measuring machine, respectively. For the surface roughness measurements, three random points on the surface of each test specimen were measured in the longitudinal direction, and an average value was calculated. The R_a was used as a parameter for the surface roughness.

In addition, the surface residual stresses of the laser-peened specimens in the longitudinal direction were measured by the cos α method using an X-ray residual stress-measuring device. The residual stress was evaluated at three points and an average was calculated. In this study, the (212) diffraction peak of Si_3N_4 was measured using the Cr-Kα characteristic X-ray line.

Furthermore, to evaluate the residual stress distribution in the depth direction, sequential polishing in the depth direction was performed. During polishing, the surface of the specimen was mirror-finished by buffing with a diamond slurry with a particle diameter of 1 μm. The amount of polishing was measured based on the change in the thickness of the specimens before and after polishing using a micrometer.

3 RESULTS AND DISCUSSION

3.1 Surface observations and surface roughness

The surface of each test specimen was observed. Figure 2 shows the optical micrographs of the surface of each specimen. There was no chipping on the edge of the smooth specimens, as shown in Figure 2(a). The micrographs in Figure 2(b) and (c) show an enlarged view of the surface on which LP was applied. The specimens that were laser peened with a power density of 16 GW/cm^2 and coverage of 1000% exhibited a partially dark and discolored surface, while the edges remained similar to that of the smooth specimens, as shown in Figure 2(b). However, surface cracks were observed on the surface of the samples laser peened with a power density of 16 GW/cm^2 or more and coverage of 3000% or more, as shown in Figure 2(c). Chipping and peeling were clearly observed at the edges of the shot-peened specimens due to the physical contact of the shot material, as shown in Figure 2(d).

Figure 3 shows the calculated R_a of each test specimen. The R_a of the laser-peened specimens increased with increasing coverage and power density. The asterisk mark in Figure 3 shows that surface cracks occurred due to LP.

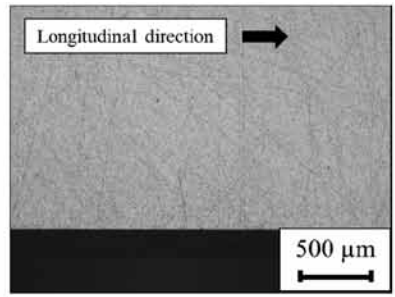

(a) Smooth (Non-LP) specimen

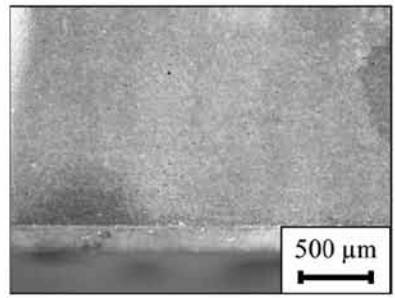

(b) Laser-peened specimen
(G = 16 GW/cm^2, C_v = 1000%)

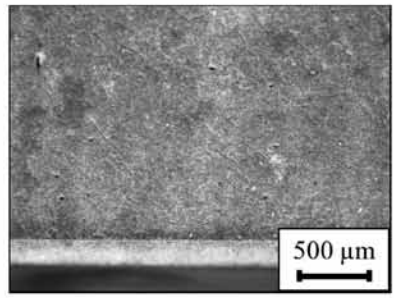

(c) Laser-peened specimen

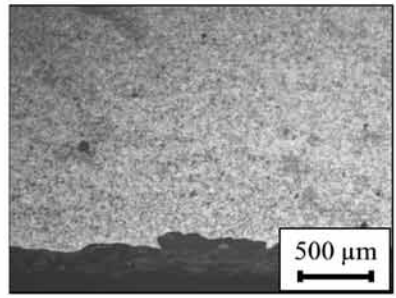

(d) Shot-peened specimen
(G = 16 GW/cm^2, C_v = 3000%)

FIGURE 2
Optical micrographs of the surfaces of the specimens.

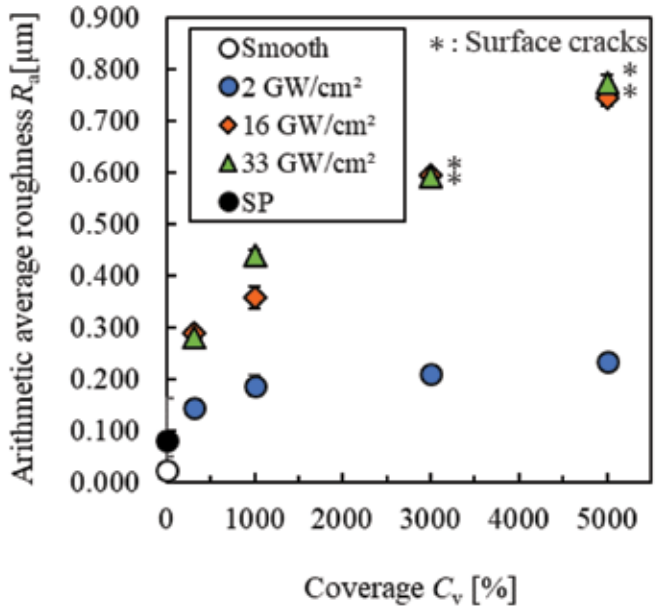

FIGURE 3
Surface roughness (R_a) of each surface-treated specimen.

3.2 Surface residual stress

Figure 4 shows the residual stresses measured at the surfaces of the specimens. Compressive residual stress was introduced by LP. The maximum compressive residual stress was about 280 MPa. The specimens that were laser peened at 16 and 33 GW/cm^2 showed much larger compressive residual stresses than those peened at 2 GW/cm^2. The asterisk mark in Figure 4 shows the occurrence of surface cracks. Surface cracks were observed on the sample when the LP parameters such as power density and coverage were too high.

3.3 Residual stress distribution from the surface in the depth direction

Figure 5 shows the residual stress distribution for each coverage. Generally, the compressive residual stress and the depth of the crossing point (i.e., the point at which the residual stress changes from compression to tension) tend to increase as the value of G increases. However, when the C_v values were 314% and 1000%, the compressive residual stress values saturated at $G = 16$ GW/cm^2. The amount of heat input increases as the value of G increases. Therefore, it was expected that the compressive residual stress would become small. When the C_v was 314%, the compressive residual stress values were smaller than those at other C_v values.

When SP was applied to Si_3N_4/SiC, the compressive residual stress on the surface was about 1500 MPa and the introduction depth was about 40 μm, as

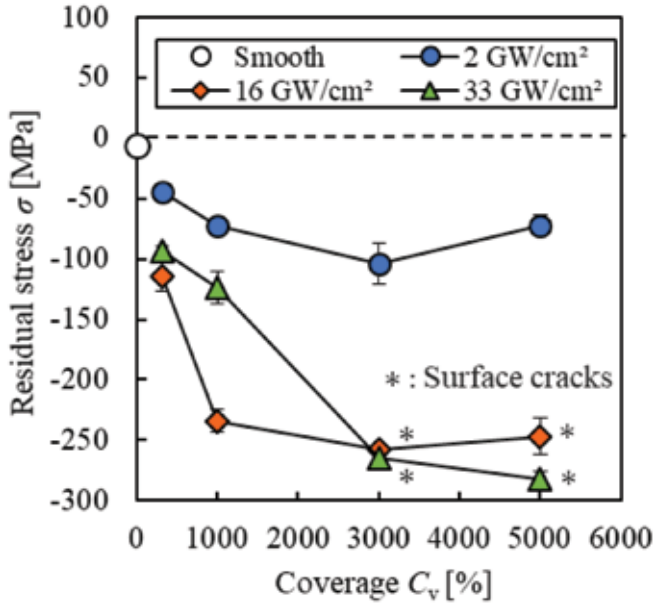

FIGURE 4
Surface residual stress at each power density and coverage.

shown in Figure 6. The residual stress of the shot-peened specimen greatly decreased and approached 0 MPa as the depth exceeded 20 μm. On the other hand, the laser-peened specimen retained the compressive residual stress even at a depth of 40 μm. From this observation, it was concluded that although the laser-peened sample had a smaller surface residual stress than the shot-peened sample, the compressive residual stress could be introduced deeper below the surface. The optimal LP conditions were found to be a G value of 16 GW/cm^2 and a C_v of 1000%. This is because the surface compressive residual stress was the largest among the specimens with no surface cracking after LP.

4 CONCLUSIONS

LPwC was applied to Si_3N_4/SiC composite materials to increase the surface strengths of the ceramics. The influences of LP on the surface conditions, surface roughness, and distribution of residual stress in the depth direction were investigated.

(1) Surface roughness increased by LP due to laser ablation. When the LP parameters such as power density and coverage were too high, surface cracks appeared on the sample.

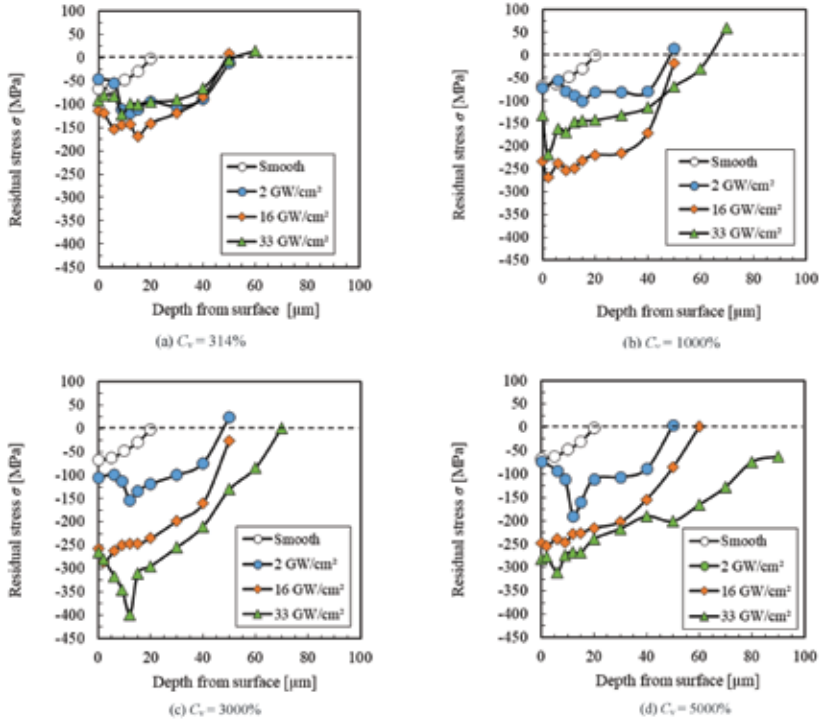

FIGURE 5
Residual stress distributions for Si_3N_4/SiC samples after LP.

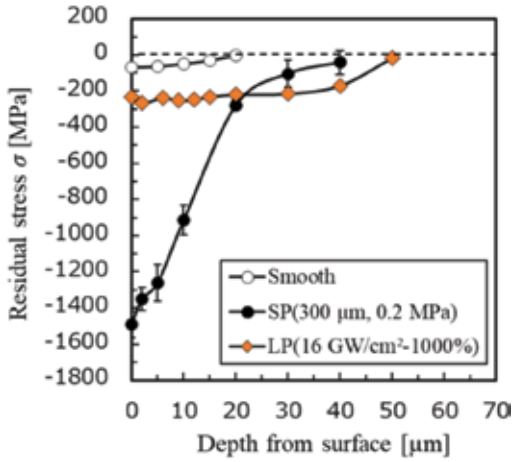

FIGURE 6
Comparison of residual stress distributions of laser-peened and shot-peened specimens.

(2) Compressive residual stresses up to 230 MPa were introduced by LP without peeling or chipping of the surface.
(3) The depth of the compressive residual stress was about 50 μm. The surface compressive residual stress of the laser-peened specimen was smaller than that of the shot-peened specimens. However, the depths of compressive residual stress in laser-peened specimens were deeper than those of the shot-peened specimens.

Nomenclature

t Pulse duration (ns)
D Spot diameter of the laser (mm)
E_p Pulse energy (mJ)
N_p Irradiation density (mm^{-2})
G Power density (GW/cm^2)
A_p Spot area (mm^2)
C_v Coverage (%)
R_a Arithmetic average surface roughness (μm)

Greek symbols

λ Wavelength of pulse laser (nm)
σ Residual stress (MPa)

ACKNOWLEDGMENT

The study was supported in part by a grant for Scientific Research (B) (16H04231) from the Ministry of Education, Culture, Sports, Science, and Technology of Japan.

REFERENCES

[1] Itoh Y., Suyama S. and Fuse T. Effect of soft shot peening on bending strength of partially stabilized zirconia. *Journal of the Ceramic Society of Japan* **111** (2003), 776–780.
[2] Moon W., Ito T., Uchimura S. and Saka H. Toughening of ceramics by dislocation subboundaries. *Materials Science and Engineering A* **387** (2004), 837–839.
[3] Tanaka K., Akiniwa Y. and Morishita Y. Residual stress distribution in the sub-surface region of shot-peened ceramics. *Transactions of the Japan Society of Mechanical Engineers Part A* **71** (2005), 1714–1721.
[4] Pfeiffer W. and Frey T. Strengthening of ceramics by shot peening. *Journal of the European Ceramic Society* **26** (2006), 2639–2645.
[5] Takahashi K., Nishio Y., Kimura Y. and Ando K. Improvement of strength and reliability of ceramics by shot peening and crack healing. *Journal of the European Ceramic Society* **30** (2010), 3047–3052.
[6] Koike H., Iwanaka K. and Takahashi K. Measurement of sliding wear of shot-peened Partially Stabilized Zirconia plate. *Applied Mechanics and Materials* **597** (2014), 353–357.

[7] Takahashi K., Iwanaka K., Osada T. and Koike H. Increase in strength of partially stabilized zirconia after shot peening. *Journal of Materials Engineering and Performance* **24** (2015), 3573–3578.

[8] Shukla P. and Lawrence J. Micro-shot peening of zirconia-advanced ceramic: an examination of surface integrity. *Journal of Material Science* **50** (2015), 1728–1739.

[9] Montross C., Wei T., Ye L., Clark G. and Mai Y. Laser shock processing and its effects on microstructure and properties of metal alloys: A review. *International Journal of Fatigue* **24** (2002), 1021–1036.

[10] Sano Y., Mukai N., Okazaki K. and Obata M. Residual stress improvement in metal surface by underwater laser irradiation. *Nuclear Instruments and Methods in Physics Research B* **121** (1997), 432–436.

[11] Sano Y., Obata M., Kubo T., Mukai N., Yoda M., Masaki K. and Ochi Y. Retardation of crack initiation and growth in austenitic stainless steels by laser peening without protective coating. *Material Science and Engineering A* **417** (2006), 334–340.

[12] Zhang X., Zhang Y., Lu J., Xuan F., Wang Z. and Tu S. Improvement of fatigue life of Ti-6Al-4V alloy by laser shock peening. *Material Science and Engineering A* **527** (2010), 3411–3415.

[13] Hatamleh O., Lyons J. and Forman R. Laser and shot peening effects on fatigue crack growth in friction stir welded 7075-T7351 aluminum alloy joints. *International Journal of Fatigue* **29** (2007), 421–434.

[14] Wang J., Zhang Y., Chen J., Zhou J., Ge M., Lu Y. and Li X. Effects of laser shock peening on stress corrosion behavior of 7075 aluminum alloy laser welded joints. *Material Science and Engineering A* **647** (2015), 7–14.

[15] Li Y., Zhou L., He W., He G., Wang X., Nie X., Wang B., Luo S. and Li Y. The strengthening mechanism of a nickel-based alloy after laser shock processing at high temperatures. *Science and Technology of Advanced Materials* **14** (2013), 055010.

[16] Akita K., Sano Y., Takahashi K., Tanaka H. and Ohya S. Strengthening of Si_3N_4 ceramics by laser peening. Material Science Forum **524** (2006), 141–146.

[17] Shukla P., Smith G., Waugh D. and Lawrence J. Development in laser peening of advanced ceramics. *International Society for Optics and Photonics* **9657** (2015), 77–85.

[18] Shukla P., Nath S., Wang G., Shen X. and Lawrence J. Surface property modifications of silicon carbide ceramic following laser shock peening. *Journal of the European Ceramic Society* **37** (2017), 3027–3038.

[19] Shukla P., Robertson S., Wu H., Telang A., Kattoura M., Nath S., Mannava S., Vasudevan V. and Lawrence J. Surface engineering alumina armour ceramics with laser shock peening. *Materials and Design* **134** (2017) 523–538.

[20] Shukla P. and Lawrence J. Laser shock peening of $S_{i3}N_4$ ceramics: Experimental set-up and general effects. Science and Technology Facilities council **40** (2014/15).

[21] Shukla P. and Lawrence J. Alteration of fracture toughness (K_{Ic}) of Si_3N_4 advanced ceramics by laser shock peening. *Science and Technology Facilities council* **41** (2014/15).

[22] Shukla P. Laser shock peening of metals and advanced ceramics. *The Laser User* **87** (2018), 24–25.

[23] Wang F., Zhang C., Lu Y., Nastasi M. and Cui B. Laser shock processing of polycrystalline alumina ceramics. *Journal of the American Ceramic Society* **100** (2017), 911–919.

[24] Wang F., Zhang C., Yan X., Deng L., Lu Y., Nastasi M. and Cui B. Microstructure-property relation in alumina ceramics during post-annealing process after laser shock processing. *Journal of the American Ceramic Society* **101** (2018), 4933–4941.

[25] Xing Y., Deng, J., Zhang, K., Zhang G. and Gao H. Effect of femtosecond laser pretreatment on wear resistance of Al_2O_3/TiC ceramic tools in dry cutting. *International Journal of Refractory Metals and Hard Materials* **43** (2014), 291–301.

[26] Ando K., Takahashi K., Nakayama S. and Saito S. Crack-healing behavior of Si_3N_4/SiC ceramics under cyclic stress and resultant fatigue strength at the healing temperature. *Journal of the American Ceramic Society* **8** (2002), 2268–2272.